

Full length article

## Formation of self-assembled monolayer of curcuminoid molecules on gold surfaces



Isadora Berlanga<sup>a,1</sup>, Álvaro Etcheverry-Berríos<sup>b</sup>, Andy Mella<sup>b</sup>, Domingo Jullian<sup>b</sup>, Victoria Alejandra Gómez<sup>a</sup>, Núria Aliaga-Alcalde<sup>c,d</sup>, Victor Fuenzalida<sup>a</sup>, Marcos Flores<sup>a,\*\*</sup>, Monica Soler<sup>b,\*</sup>

<sup>a</sup> Departamento de Física, Facultad de Ciencias Físicas y Matemáticas, Universidad de Chile, Av. Blanco Encalada 2008, Santiago, Chile

<sup>b</sup> Departamento de Ciencia de los Materiales, Facultad de Ciencias Físicas y Matemáticas, Universidad de Chile, Beaucheff 851, Santiago, Chile

<sup>c</sup> ICREA (Institució Catalana de Recerca i Estudis Avançats), Passeig Lluís Companys, 23, 08018, Barcelona, Spain

<sup>d</sup> CSIC-ICMAB (Institut de Ciència dels Materials de Barcelona), Campus de la Universitat Autònoma de Barcelona, 08193 Bellaterra, Spain

### ARTICLE INFO

#### Article history:

Received 13 May 2016

Received in revised form 8 September 2016

Accepted 17 September 2016

Available online 18 September 2016

#### Keywords:

Curcumin derivatives

Curcuminoid

XPS

STM

Polycrystalline gold surface

Self-assembled monolayers (SAMs)

### ABSTRACT

We investigated the formation of self-assembled monolayers of two thiophene curcuminoid molecules, 2-thphCCM (**1**) and 3-thphCCM (**2**), on polycrystalline gold substrates prepared by immersion of the surfaces in a solution of the molecules during 24 h. The functionalized surfaces were studied by scanning tunneling microscopy (STM) and X-ray photoelectron spectroscopy (XPS). Despite the fact that both molecules have the same composition and almost the same structure, these molecules exhibit different behavior on the gold surface, which can be explained by the different positions of the sulfur atoms in the terminal aromatic rings. In the case of molecule **1**, the complete formation of a SAM can be observed after 24 h of immersion. In the case of molecule **2**, the transition from flat-lying to upright configuration on the surface is still in process after 24 h of immersion. This is attributed to the fact that molecule **2** have the sulfur atoms more exposed than molecule **1**.

© 2016 Elsevier B.V. All rights reserved.

### 1. Introduction

The ability to deposit single molecules as building blocks on surfaces and understanding their morphology represents one of the main challenges for the design of molecular devices for future technological applications [1]. The formation of self-assembled monolayers of molecular systems with coordinating atoms to bind the surfaces is a simple, controllable and effective bottom-up approach for the preparation of molecular arrays on surfaces at the nanometer scale. They can be prepared by immersion of the surface in the molecular solution or via vapor phase deposition of the molecules under UHV conditions [2]. The adsorption of

organosulfur molecules on solid metal surfaces from organic solvents, for example thiols on gold surfaces, gives rise to ordered self-assembled monolayers (SAMs) [3–10]. In particular, there are several studies of SAMs of alkanethiols [11,12] used as organic surfaces in a broad variety of applications, such as lubrication, corrosion inhibition, electrochemistry and biotechnology [3].

The formation of self-assembled monolayers of  $\pi$ -conjugated aromatic compounds, such as thiophene derivatives, have also been studied due to their optical and electrical properties, which make them appealing for optoelectronic devices [13]. Nevertheless, there are still many unsolved questions concerning the chemical state and interaction of thiophene groups and gold surfaces [14,15]. There are many papers discussing the molecule-surface interaction of alkanethiol molecules on gold surfaces, but only few papers discuss the binding of thiophene and thiophene derivatives on gold surfaces [15–21]. If one considers the different electronic structures of alkanethiol and thiophene molecules, the binding with a gold surface should be different. The sulfur atom in alkanethiols as well as in thiophenes has unpaired electrons, which can bind to the gold surface. However, in thiophenes the sulfur atom is part of a conjugated aromatic ring, allowing bonding to the surface through the  $\pi$ -system. Therefore, unlike the flexible interaction of the thiolate

\* Corresponding author at: Departamento de Ciencia de los Materiales, Facultad de Ciencias Físicas y Matemáticas, Universidad de Chile, Beaucheff 851, Santiago, Chile.

\*\* Corresponding author at: Departamento de Física, Facultad de Ciencias Físicas y Matemáticas, Universidad de Chile, Av. Blanco Encalada 2008, Santiago, Chile.

E-mail addresses: [mflorescarra@ing.uchile.cl](mailto:mflorescarra@ing.uchile.cl) (M. Flores), [msoler@ing.uchile.cl](mailto:msoler@ing.uchile.cl) (M. Soler).

<sup>1</sup> Present address: Department of Earth & Planetary Sciences, Harvard University, 100 Edwin H. Land Blvd., Cambridge, MA, 02142-1204, USA.

linkage to the metal surface, giving ordered SAMs, small changes in the ring orientation of the thiophene relative to the metal surface will strongly modify the sulfur-gold bonding interaction [22].

STM studies of thiophene molecules deposited by immersion on gold surfaces showed the formation of a stable SAM, as reported for alkanethiol molecules [23]. The interpretation of the XPS S 2p spectra of thiophene and thiophene derivatives on gold surfaces is not direct, being the assignment of the sulfur-gold binding energy peaks object of some discussion in the literature. Most authors agree that the S1 and S2 peaks, at 161 and 162 eV, are attributed to sulfur from the thiophene ring bound to the gold surface with no dissociation of the ring [15–21]. S3 and S4 peaks, at 163 and 164 eV, have been mainly reported in the S2p spectra of thiophene derivatives on gold, being assigned to unbound sulfur [15]. In this paper, we use STM and XPS to examine the molecular arrangement of two bithiophene curcuminoid molecules deposited on gold surfaces by immersion in the molecular solution, trying to understand their interaction with the gold surface.

## 2. Experimental and computational details

### 2.1. Synthesis and characterization of 2- and 3-thphCCM

The materials for the synthesis of 2-thphCCM (**1**) and 3-thphCCM (**2**) were purchased from Sigma-Aldrich and Merck and were used without any additional purification. Gold shot was purchased from Alfa Aesar, with a purity of 99.9999%. Mica Muscovite surfaces were commercially purchased from Mica and Micanite Supplies Ltd. Methanol was purchased from Merck.

Preparation of ((1E,4Z,6E)-5-hydroxy-1,7-di(thiophen-2-yl)hepta-1,4,6-trien-3-one) (2-thphCCM, **1**) and ((1E,4Z,6E)-5-hydroxy-1,7-di(thiophen-3-yl)hepta-1,4,6-trien-3-one) (3-thphCCM, **2**) were done following the same synthetic methodology as previously reported [24]. In order to characterize the bulk samples of 2-thphCCM (**1**) and 3-thphCCM (**2**) several techniques were used: C, H and S analyses were performed with a Perkin-Elmer II Series CHNS/O Analyzer 2400 at the Servei de Microanàlisi del Consell Superior d'Investigació Científiques (CSIC), Barcelona; <sup>1</sup>H NMR and <sup>13</sup>C NMR spectra was recorded on a Bruker Avance-400 spectrometer; The ESI mass spectra were performed with a spectrometer LC/MSD-TOF (Agilent Technologies) with double nebulizer source; Infrared spectra (4000–400 cm<sup>-1</sup>) were recorded from KBr pellets on a Bruker Vector 22 spectrophotometer. Characterization details are presented in Table S1.

### 2.2. Surface and preparation

Gold films of high purity (99.9999%) were deposited on freshly exfoliated Muscovite mica by physical method using a resistively heated tungsten basket. A quartz balance located close to the sample monitored the thickness of the deposited film. Depositions were performed in a high vacuum system (10<sup>-4</sup> Pa); keeping the substrate temperature at 300 °C with an evaporation rate of 1.2 nm/min. The resulting Au film thickness was 35 nm. Finally, the surfaces were eroded with Ar<sup>+</sup> ions at 2 keV for 10 min. In order to guarantee the cleanliness of the surfaces, particularly regarding sulfur impurities, STM and XPS measurements were performed before and after erosion with Ar<sup>+</sup> ions. Fig. S1 shows the STM topography scans of control experiments of the gold polycrystalline surfaces.

### 2.3. STM/XPS sample preparation

The X-ray photoelectron spectroscopy measurements (XPS) were carried out at room temperature using a Physical Electronics 1257 system with a hemispherical analyzer and non-

monochromatized radiation (Al-K $\alpha$ , 1486.6 eV) operating at 200 W with working pressures in the range of 10<sup>-6</sup>–10<sup>-7</sup> Pa and using high resolution scans (pass energy 44.75 eV and step size 200 meV). The spectra of the pure gold surface were calibrated to the Au 4f<sub>7/2</sub> core level binding energy at 84.0 eV. In order to detect all the elements on the surface, a survey scan of each sample was recorded before acquiring the high resolution spectra. The XPS spectra were adjusted using the CASA XPS program with a Gaussian-Lorentzian mix function and Shirley background subtraction.

STM images were acquired with an Omicron UHV AFM/STM operating at room temperature in high vacuum conditions. STM measurements were performed in constant current mode with mechanically formed Pt-Ir tips. The images were processed using WSxM [25].

### 2.4. Preparation of films of molecule 1 and 2 on gold surfaces

Gold surfaces were immersed in 1 mM solution of molecules **1** and **2** in methanol for 1 h, 8 h, 12 h and 24 h. Thereafter, the samples were washed with methanol and dried under a flow of N<sub>2</sub>. All experiments were characterized immediately in order to avoid further contamination. Fig. S4 presents the XPS spectra of the Au surface after immersion in methanol as a control. Fig. S5 is a broad spectrum of a gold surface after immersion showing the dominant Au signal as well as the C 1s and O 1s; the broad spectrum seems similar for both molecules. Fig. S6 shows the XPS spectrum of C 1s spectrum of (a) 2-thphCCM (**1**) and (b) 3-thphCCM (**2**) as a function of immersion time.

### 2.5. Computational details

The calculations were performed using the SDA version 6 software [26] and VMD [27] software for molecular visualization. Density functional theory (DFT) calculations have been used to provide molecular insights into the curcuminoids-gold interactions that are not accessible from experiments alone. SDA 6.0 package was used to simulate the Au polycrystalline surface. The Au surface was simulated using an area of 100 Å × 100 Å and three atomic layers. The first layer corresponds to 2760 virtual sites, which restrict the ligand in front of gold atoms [28], and the other two layers with 1307 atoms. The force field used for the simulation is the GolP [29,30], which is constructed taking into account the polarization effects of gold [31].

## 3. Results and discussion

One of the objectives of this article is the design of thiophene derivative materials with a wide range of physical and chemical properties, as well as tunable architectures. This can be envisioned by introducing selected organic fragments containing groups with sulfur coordinating atoms, with the goal of binding to a gold surface. The experiments presented in this work are based on the formation of molecular films on gold surfaces using two bithiophene curcuminoid molecules (derivatives from curcumin) [23]. Curcuminoid molecules are  $\pi$ -conjugated systems based on diaryl-heptanoid chains, with a central  $\beta$ -diketone moiety, which can be coordinated with metal ions, and two terminal aryl groups, which can be easily modified to improve the electrical contact with surfaces or electrodes (eg.; thiophene) [32,33]. The ones selected for this work have terminal thiophene groups with different coordinating directions, as presented in Fig. 1. Although some examples of curcuminoid molecules on surfaces have been published, well-ordered arrangements of curcuminoid molecules on gold surfaces still remain unexplored [34]. Some of us have reported on the growth of anthracene curcuminoid arrays on highly oriented pyrolytic graphite (HOPG) substrates by dip-coating deposition or

by spin-coating [35]. These curcuminoid ligands on surface may provide electronic and fluorescent properties at the nanoscale level.

The organization of these two thiophene-curcuminoid molecules on gold surfaces has been followed by STM and XPS. The selection of both curcuminoid molecules 2-thphCCM, (**1**) and 3-thphCCM, (**2**) shown in Fig. 1, relies on the different position of the sulfur atom in the terminal thiophene rings. This leads to two different possible interactions with the gold surface after deposition and growth of the thin films. These interactions will depend on the availability of the sulfur atoms to bind the metal surface, possibly influencing the angle and density of such molecules at the surface. Fig. 2 shows the two possible arrangements of molecule **1** and **2** on a gold surface, flat-lying (left) and upright (right), respectively. In Fig. 2,  $\theta$  is the angle between the surface and the long axis of the molecule.

In order to identify the preferred orientations of molecules **1** and **2** close to the surface, based on Coulomb interactions, before any other binding interactions enter into play, simulations of the molecular arrangement as the molecules approach to the surface, just before adsorption, were performed. The calculation used the docking modeling and does not consider the sulfur-gold surface interaction, but it provides a first order approximation for the arrangement of the molecule as it approaches the surface. These modeling studies of the curcuminoid-Au system yielded preferentially the flat-lying configuration, accounting for about 90% of the probability in the case of both molecules (Fig. 3), in the early stages of the adsorption process.

The gold polycrystalline substrates were prepared by vacuum deposition, as described in a previous paper [36] with subtle modifications, as described in the experimental section. The single grains and grain boundaries of the polycrystalline gold films are identified by STM in Fig. 4 showing grain sizes between 30 and 100 nm. Increasing the substrate temperature induces growth of the grain size, thus providing flat terraces suitable to anchor organic molecules able to develop self-assembled monolayers (SAMs). For the deposition of the molecules, the gold surfaces were immersed in 1 mM methanol solution of 2-thphCCM (**1**) or 3-thphCCM (**2**) for 24 h. Afterwards, the surfaces were rinsed with methanol, dried with a flow of nitrogen and analyzed by STM and XPS. A time evolution study has also been performed to try to understand the

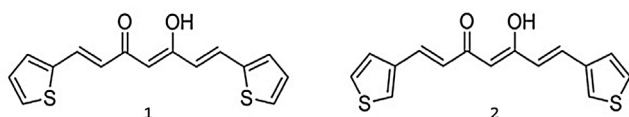


Fig. 1. Thiophene-curcuminoid molecules, 2-thphCCM (**1**) (left) and 3-thphCCM (**2**) (right).

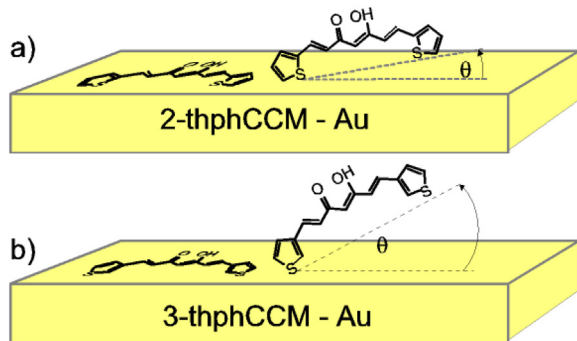


Fig. 2. Schematic view of the two configurations of molecules **1** (top) and **2** (bottom) on a surface, flat-lying (left) and upright (right), respectively.  $\theta$  is the angle between the long axis of the molecule and the surface. The angle between the plane of the molecule and the surface is not shown for simplicity.

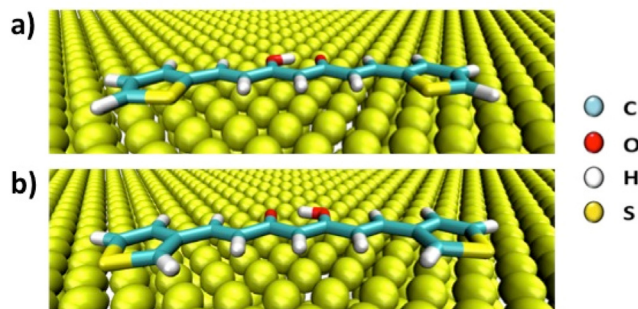


Fig. 3. Molecular docking prediction of the most stable position based on coulombic interactions of molecule **1** (top) and **2** (bottom) on a gold surface.

formation of the molecular films, by preparing samples following the same procedure but changing the immersion times to 1 h, 8 h and 12 h (Fig. S2–S3).

The topographic images of the films after immersion of the gold surfaces in a methanol solution of molecule **1** (top) and **2** (bottom) for 24 h as measured by STM are shown in Fig. 4. The left side of the figure shows low magnification images, exposing the grain structure of the deposited film. The right side of the figure presents a magnification of the region inside the rectangle of the left side, corresponding to the image of the flat areas inside a single grain. The inset in the right figure shows a line profile, which is related with the corrugation. This parameter is associated to the height differences in the surface. In our case, we use this line profile to quantify the level of organization of the molecules in the surface. We identify higher values of corrugation with molecules in different configurations, thus with different heights on the surface. In the same way, lower values imply mainly a more uniform configuration [37]. By following this parameter we can discuss the evolution of the different configurations. For the molecule **1** film (Fig. 4b) obtained after 24 h immersion of the surface in the molecular solution, the nominal height of 1–2 Å can correspond to: (1) adsorbed molecules with the long axis nearly parallel to the substrate surface in a flat-lying configuration; (2) molecules with a small angle or (3) well ordered SAMs of low roughness. For molecule **2** (Fig. 4d) a higher roughness is observed, with a nominal height in the inset of almost 6–7 Å, suggesting that most of the molecules are in the upright configuration with different inclinations. In neither of the films an organized self-assembled monolayer was directly observed by STM. The higher corrugation observed for molecule **2** is consistent with its structure, which allows adsorption at larger angles, due to fewer steric constraints.

The time evolution of the STM images of the films prepared at different immersion times for molecule **1** and **2** exhibit some differences, as shown in Figs. S2–S3. In the case of the films based on **1**, the height differences in the inset starts with 2 Å after one hour, increases to a maximum of 5 Å after 12 h of immersion, and decreases again to 2 Å again after 24 h. This suggests fluctuations between smaller and larger angles or between flat-lying and upright at different angles at different immersion times, until a more regular and dense molecular array is formed after 24 h. In the case of molecule **2**, the height differences in the line scan start at 2 Å after one hour, increasing to 7 Å after 24 h. This means that the film is still under organization, with a mixture of configurations, not yet forming a SAM. Complementary information about the organization of the molecules on the surface is provided by the XPS analysis.

In order to understand the interaction and arrangement of molecules **1** and **2** on the gold surfaces, XPS measurements of the deposits of 2-thphCCM (**1**) and 3-thphCCM (**2**) were performed. A survey recorded in the energy range of 0–600 eV (Fig. 5) is dom-



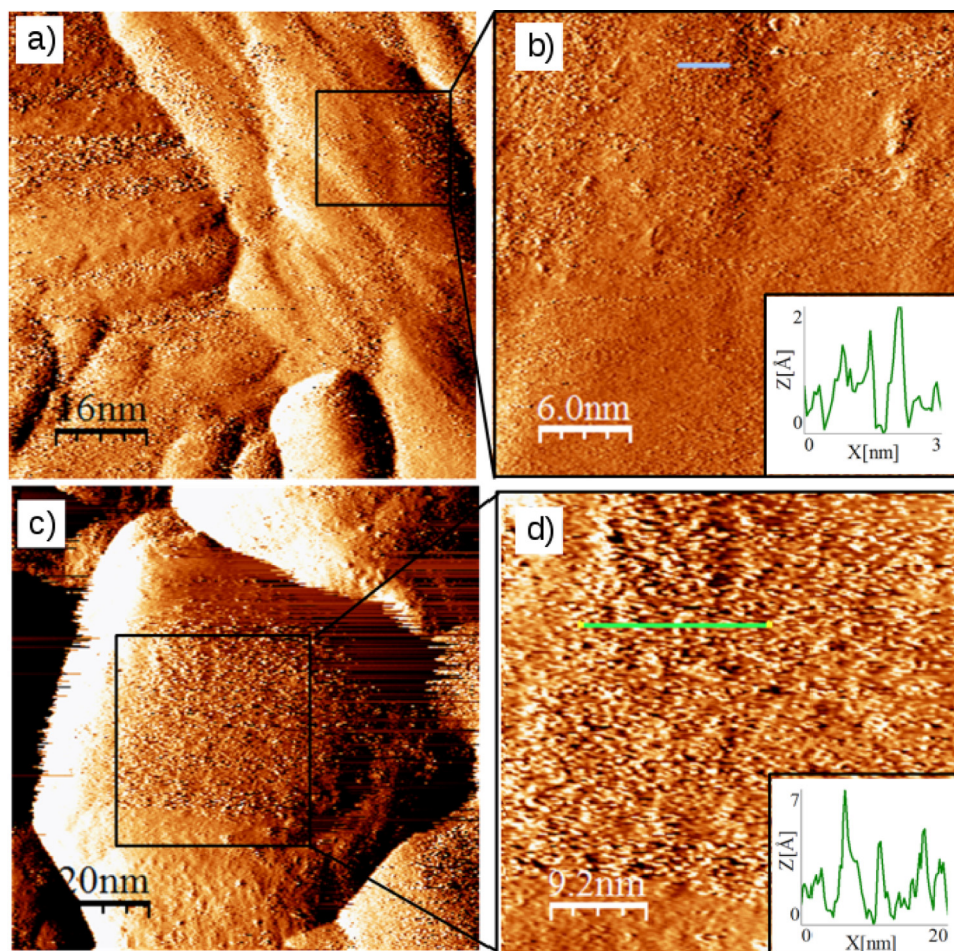


**Fig. 4.** STM topography scan of the films of molecule **1** (a and b) and molecule **2** (c and d) on a polycrystalline gold a surface after an immersion of 24 h in the molecular solutions. The right pictures (b and d) are higher magnification images recorded from the region inside the rectangle of the left. The inset at the right is a line scan used to evaluate the corrugation.

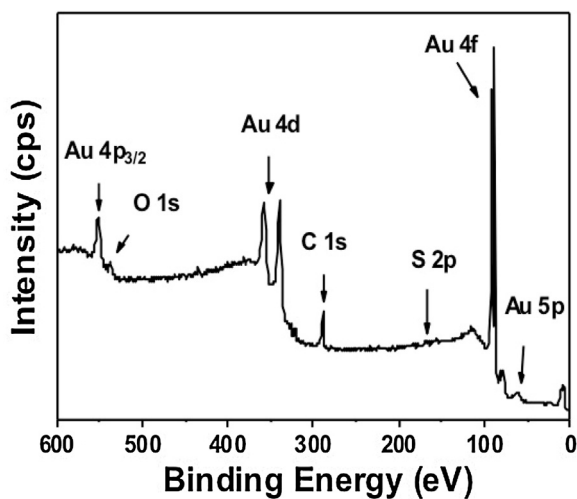


**Fig. 5.** Representative XPS survey spectrum of a curcuminoid molecule on a polycrystalline Au substrate measured after 24 h immersion.

inated by the strong peaks originated from Au 4f photoelectrons and shows additional signals from C 1s and O 1s. The S 2p signal cannot be observed in the scale of the figure but it is shown in the high resolution spectra. In the case of C 1s and O 1s core levels, we observed binding energies and line shapes consistent

with the chemical structure and the stoichiometry expected for the molecules adsorbed with no modification (Fig. S2). We restrict the discussion to the sulfur 2p levels presented in Fig. 6.

The S 2p spectra are composed of  $2p_{3/2}$  and  $2p_{1/2}$  peaks with an intensity ratio of 2:1 and a peak separation of 1.2 eV [38]. Therefore only the energy position of the stronger S  $2p_{3/2}$  peak is used in the discussion. Fig. 6 shows sulfur high-resolution XPS spectra of deposits of molecule **1** (Fig. 6a) and molecule **2** (Fig. 6b) formed after immersion of the gold surfaces in the methanol solutions of molecules **1** or **2**, respectively. Both S 2p spectra consist principally of five components labeled S1, S2, S3, S4 and S5 with binding energies differing no more than 0.2 eV between the two samples. The full width at half-maximum (FWHM) was between 0.9 and 1.2 eV. Table 1 shows the summary of reported peak assignments for the S 2p spectra of thiophene and selected thiophene derivatives.

The interpretation of the chemical condition related to the five components (S1, S2, S3, S4 and S5) of the S 2p spectra of thiophene or thiophene derivatives on gold surfaces has been discussed in the literature. Table 2 shows the summary of reported peak assignments for the S 2p spectra of thiophene and selected thiophene derivatives. The first report concerning the XPS data of thiophene derivative molecules adsorbed onto a gold surface was published by Ishida et al. who studied the high resolution XPS spectrum of a bithiophene monolayer [15]. They observed a broad S 2p spectrum consisting of three sulfur species: two S  $2p_{3/2}$  peaks at 161 eV and 162 eV assigned to two bound adsorptions of the bithiophene molecule, and one peak at 163 eV peak assigned to an unbound

**Table 1**  
Binding Energy (eV) of the constituents of the S 2p<sub>3/2</sub> photoelectron signal and their interpretation.

Peak id	Bisthiophene [15]	Thiophene [17]	Thiophene/ $\alpha$ -bithiophene [18]	Thiophene [19]	Thiophene/dimethylthiophene [21]	Molecules 1 and 2 (this work) $\pm 0.2$ eV	Interpretation: bound or unbound to the surface
S1	161.1	161.0	–	–	161.0/161.0	161.2	Bound, <b>flat-lying</b>
S2	162.0	162.0	162/-	–	162.0/162.0	161.8	Bound, <b>upright</b>
S3	163.7	–	-/163.4 <sup>a</sup>	163.8	-/163.4	163.8	Unbound
S4	–	–	–	164.5	-/164.2	164.5	Unbound
S5	–	–	–	–	–	167.2	–

Fig. 2 shows the two possible arrangements of molecule 1 and 2 on a gold surface, flat-lying (left) and upright (right), respectively. The significance of the bold is to emphasize the two arrangements.

<sup>a</sup> Sulfur condition not assigned in the publication.

**Table 2**  
Intensities associated to the first four peaks of the S 2p spectra after 24 h of immersion. The S5 (oxidized sulfur) peak is not considered here.

Peak id	Relative intensity%		Sulfur condition	% of bound and unbound sulfur	
	2-thphCCM (1)	3-thphCCM (2)		2-thphCCM (1)	3-thphCCM (2)
S1	0	5	Bound sulfur	42 $\pm$ 6 <sup>a</sup>	37 $\pm$ 4 <sup>a</sup>
S2	42	32			
S3	50	29	Unbound sulfur	58 $\pm$ 6 <sup>a</sup>	63 $\pm$ 4 <sup>a</sup>
S4	8	34			

<sup>a</sup> Estimated error.

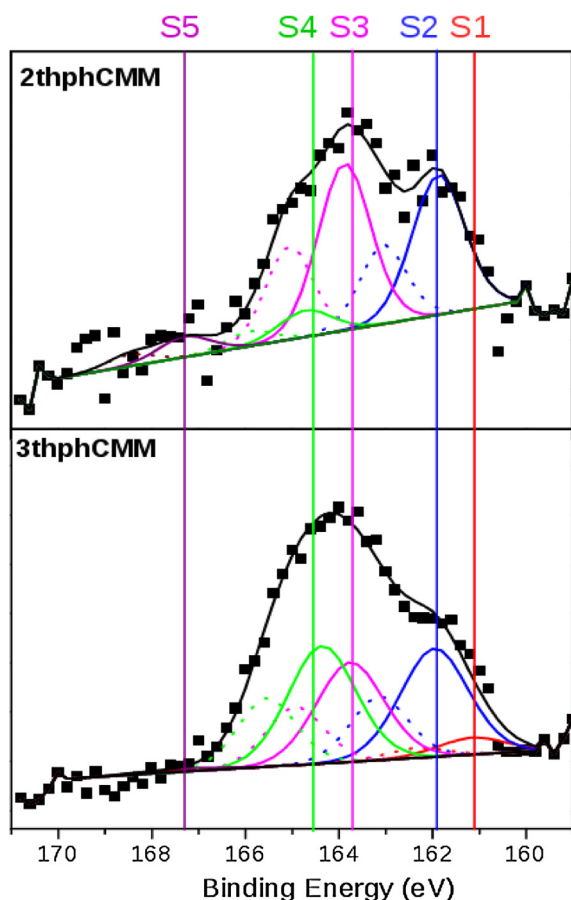


**Fig. 6.** XPS spectra of the sulfur 2p core level from films grown of molecule 1 (top) and molecule 2 (bottom) on Au surface after 24 h of immersion in the solution. S1 and S2 correspond to bound sulphur whereas S3 and S4 to unbound, while S5 is an oxidized state. The full lines are the fittings of the 2p<sub>3/2</sub> peaks and the dotted lines are the corresponding 2p<sub>1/2</sub>. The squares are the experimental points and the solid black line joining them the fitting.

sulfur atom of the bithiophene molecule. Since the bithiophene molecule has two sulfur atoms, they assigned the 162 eV peak to the sulfur bound to the surface, and the 163 eV peak to unbound sulfur of the same molecule in a SAM arrangement [15], similar to dithiol molecules reported by Rieley et al. [39].

Noh et al. reported the first XPS spectra of single thiophene molecules on gold surfaces, assigning the S 2p<sub>3/2</sub> peak at 162 eV to the sulfur atom bound to the surface in an upright configuration, forming SAMs, similar to the peaks of the alkanethiols. They assigned the lower binding energy peak at 161 eV to the  $\pi$ -conjugated interaction between the sulfur-aromatic ring and the surface in a flat-lying configuration [17]. Ito et al. reported lower resolution XPS spectra of a thiophene molecule on a gold surface, showing only the S 2p<sub>3/2</sub> peak of the bound sulfur peak located at 162 eV (S2), which was associated again to a chemisorbed state suggesting the formation of a SAM. In the same article, they reported a different adsorption state for the bithiophene, exhibiting a main peak around 163.4 eV (S3), which they assigned to the sulfur atoms interacting weakly with the gold surface [18,20]. In the same year, Nambu et al. report on physisorbed thiophene on gold at low temperatures identifying a sulfur S 2p<sub>3/2</sub> peak at 163.8 eV at low coverage, an energy consistent with S3 [19]. The peak moved to higher values when increasing the coverage, reaching 164.5 eV (S4) above 2.4 monolayers. They attributed this shift to the decreasing screening effect of the electrons in the metal substrate, thus identifying the 164.5 eV peak with sulfur in the thiophene not bound to the surface. Their NEXAFS measurements associated the S3 peak with flat-lying molecules not bound to the surface, and the S4 to standing up arrays of molecules that were not bound to the surface, as shown by thermal desorption experiments [19].

Noh et al. in a different article compare thiophene and 2,5-dimethylthiophene on gold. They assigned the S1 and S2 peaks to chemisorbed thiophene, the first associated to a flat-lying and the second to an upright configuration, with no S3 or S4 signals. In particular, they reported the growth of thiophene molecules from solution onto a gold surface as dominated by an upright configuration of thiophene molecules, with the rest in a flat-lying configuration. In the case of 2,5-dimethylthiophene films, they observed weak S1 and S2 bound intensities but strong unbound S3 and S4 peaks. These adsorption peaks have been influenced by the

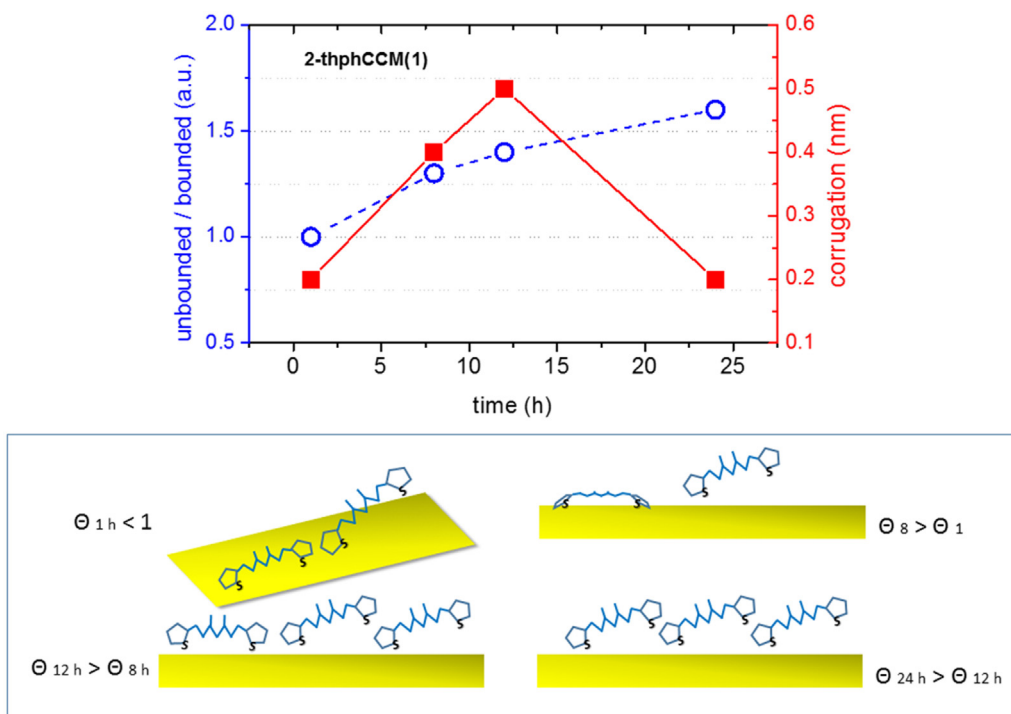


**Fig. 7.** (Top) Correlation between the XPS S 2p signal (S3+S4)/(S1+S2) ratio of molecule 1 and the evolution of corrugation as a function of the immersion time. (Bottom) Representation of the evolution of the molecular arrangement on the surface.

two methyl groups at 2,5-positions in the thiophene ring, preventing the upright configuration, showing some interactions between the  $\pi$ -system of the molecule and the gold surface. This is consistent with the steric constraint imposed by the methyl groups, diminishing the direct interaction between the sulfur and the surface, either in flat-lying or upright configurations, thus precluding the growth of SAMs [21]. The S5 peak corresponds to an oxidized component [38], the intensity of which fluctuates between 0% and 14% with an average of 6%, see SI. This does not correlate with the immersion time and can be due to the experimental preparation.

The relative intensities associated with the two bound and two unbound sulfur states after depositing molecules 1 and 2 are shown in Table 2. It includes the percent of bound and unbound sulfur of each sample. The sulfur states found in molecules 1 and 2 are the same, and are similar to the values found in the literature within the experimental error [15–21]. The small amount of S1 indicates no significant presence of flat-lying configurations after 24 h immersion. Therefore, in this case both molecules should be mainly in an upright position after 24 h of immersion. Since both molecules have one sulfur atom at each end of the molecule, they should have similar amounts of bound and unbound sulfur atoms, if a SAM with upright configuration is grown, as seen in ref [15]. In our XPS measurements the ratio between unbound and bound molecules is larger than one. However, this is consistent with the ratio between the amount of bound and unbound, since the bound sulfur signal from the surface is partially screened while photoelectrons traverse the film to reach the detector.

The temporal dependence of the intensities associated to peaks S1–S5 is available in Table S2, after immersion times of 1, 8, 12 and 24 h. The observed energy positions of the five peaks do not depend on the immersion time within the experimental error of 0.2 eV. In the case of molecule 1, the intensity of the bound sulfur S1 (flat lying [17,21]) decreases monotonically with increasing time. This correlates with the amount of oxidized sulfur, since the addition S1+S5 remains approximately constant. There is not enough data to assess if the correlation is accidental or a tendency. These ten-

dencies are not so clear for molecule 2. In molecule 2, S2 exhibits a slight increment suggesting a gradual building of a SAM, which seems to form at an earlier stage than in molecule 1.

Fig. 7 relates the temporal evolution of the XPS S 2p unbound/bound ratio of molecule 1 and its corrugation obtained from the STM images. Our interpretation suggests an incomplete molecular coverage after 1 h, where the molecules are mainly in the flat-lying configuration. The corrugation increases with the immersion time, up to 12 h, due to the transition from flat-lying to upright configuration. At 24 h, the lower corrugation suggests that the molecules are more organized, mainly all in the upright configuration, suggesting no significant differences in height. The XPS S 2p signal ratio between the unbound and bound sulfur (S3+S4)/(S1+S2) in the figure indicates an increase of the unbound sulfur with increasing immersion time. This value agrees with the observation of the transition of the molecules from flat-lying to upright configuration, and is consistent with the fact that when the molecules are in an upright position, the molecules partially screen the bound sulfur signal. Therefore, less bound sulfur signal will be measured.

Regarding the time evolution of the XPS spectra of 3-thphCCM (2) (Fig. S7) the corrugation increases with the immersion time, suggesting a transition from flat-lying to upright configuration. However, the time evolution of the corrugation does not correlate well with the evolution of the unbound/bound ratio of the XPS S 2p signals.

## 5. Conclusions

Functionalized surfaces with molecule 1 and 2 were studied by scanning tunneling microscopy (STM) and X-ray photoelectron spectroscopy (XPS). By assigning the different components of the XPS S 2p signals, based on previous reports from the literature, we discuss the different molecule configurations on the surface. These different S 2p components and their unbound/bound ratio have been correlated with the changes of corrugation measured from



the STM images. Based on these STM and XPS studies, we show that despite the similar structure of molecules 1 and 2, they exhibit a markedly different behavior on a gold surface. Both molecules may form SAMs, but due to the different position of the sulfur atom on the terminal aromatic rings, the time evolution is different. In the case of molecule 1, after 24 h of immersion, the small corrugation indicates the formation of a SAM. In the case of the film of molecule 2, after 24 h of immersion, the transition from flat-lying to upright configuration is still in process. Molecule 2 has the sulfur atoms more exposed allowing larger tilt angles when bound to the surface. In this situation, the corrugation of the deposits after 24 h is related to different arrangement of the molecules with different angles with respect to the gold surface. Therefore, due to the mixture of molecules with higher range of tilted angles, no decrease of the corrugation is observed, as seen in the case of molecule 1.

### Acknowledgements

This work has been partially financed by the Chilean government under grant PIA-ACT1117 and Fondecyt Projects 1110206, 1140759 and 3150014. Dr. N. A.-A. thanks to the MINECO (Ref: MAT2013-47869-C4-2-P), Mr. A. E.-B. acknowledges the scholarship for his PhD through Conicyt PFCHA grant 21140734. This research was also partially supported by the supercomputing infrastructure of the NLHPC (ECM-02) (Powered@NLHPC).

### Appendix A. Supplementary data

Supplementary data associated with this article can be found, in the online version, at <http://dx.doi.org/10.1016/j.apsusc.2016.09.077>.

### References

- [1] L. Sun, Y.A. Diaz-Fernandez, T.A. Gschneidner, F. Westerlund, S. Lara-Avilab, K. Moth-Poulsen, *Chem. Soc. Rev.* 43 (2014) 7378–7411.
- [2] C. Vericat, M.E. Vela, G. Benitez, P. Carro, R.C. Salvarezza, *Chem. Soc. Rev.* 39 (2010) 1805–1834.
- [3] J.C. Love, L.A. Estroff, J.K. Kriebel, R.G. Nuzzo, G.M. Whitesides, *Chem. Rev.* 105 (2005) 1103–1169.
- [4] B. O'Rourke, M. Flores, Y. Yamazaki, V. Esaulov, *Nucl. Instrum. Methods Phys. Res.: B* 68 (2013) 68–70.
- [5] M. Flores, B. O'Rourke, Y. Yamazaki, V. Esaulov, *Phys. Rev.: A* 79 (2009) 022902–022907.
- [6] R.G. Nuzzo, D.L. Allara, *J. Am. Chem. Soc.* 105 (1983) 4481–4483.
- [7] M.M. Wakzak, C. Chung, S.M. Stole, C.A. Widrig, M.D. Porter, *J. Am. Chem. Soc.* 113 (1991) 2370–2378.
- [8] P.E. Laibinis, G.M. Whitesides, D.L. Allara, Y. Tao, A.N. Parikh, R.G. Nuzzo, *J. Am. Chem. Soc.* 113 (1991) 7152–7161.
- [9] H. Ohno, L.A. Nagahara, S. Gwo, W. Mizutani, H. Tokumoto, *Mol. Cryst. Liq. Cryst.: A* 295 (1997) 189–192.
- [10] M.R. Linford, C.E.D. Chidsey, *J. Am. Chem. Soc.* 115 (1993) 12631–12632.
- [11] C.D. Bain, E.B. Troughton, Y.T. Tao, J. Evall, G.M. Whitesides, R.G. Nuzzo, *J. Am. Chem. Soc.* 111 (1989) 321–335.
- [12] P.E. Laibinis, G.M. Whitesides, D.L. Allara, Y.T. Tao, A.N. Parikh, R.G. Nuzzo, *J. Am. Chem. Soc.* 113 (1991) 7152–7167.
- [13] S. Natarajan, S.H. Kim, *Langmuir* 21 (2005) 7052–7056.
- [14] J.L. Garcia, B.J.V. Tongol, S.-L. Yau, *Electrochim. Acta* 71 (2012) 302–309.
- [15] T. Ishida, N. Choi, W. Mizutani, H. Tokumoto, I. Kojima, H. Azebara, H. Hokari, U. Akiba, M. Fujihira, *Langmuir* 15 (1999) 6799–6806.
- [16] M.H. Dishner, P. Taborek, J.C. Hemminger, F.J. Feher, *Langmuir* 14 (1998) 6676–6680.
- [17] J. Noh, E. Ito, K. Nakajima, J. Kim, H. Lee, M. Hara, *J. Phys. Chem.: B* 106 (2002) 7139–7141.
- [18] E. Ito, J. Noh, M. Hara, *Jpn. J. Appl. Phys.* 42 (2003) L852–L855.
- [19] A. Nambu, H. Kondoh, I. Nakai, K. Amemiya, T. Ohta, *Surf. Sci.* 530 (2003) 101–110.
- [20] E. Ito, J. Noh, M. Hara, *Surf. Sci.* 602 (2008) 3291–3296.
- [21] J. Noh, E. Ito, T. Araki, M. Hara, *Surf. Sci.* 532–535 (2003) 1116–1120.
- [22] J. Zhou, Y.X. Yang, P. Liu, N. Camillone, M.G. White, *J. Phys. Chem. C* 114 (2010) 13670–13677.
- [23] M.H. Dishner, J.C. Hemminger, F.J. Feher, *Langmuir* 12 (1996) 6176–6178.
- [24] A. Etcheverry-Berrios, I. Olavarria, M.L. Perrin, R. Diaz-Torres, D. Jullian, I. Ponce, J.H. Zagal, J. Pavez, S.O. Vásquez, H.S.J. van der Zant, D. Dulić, N. Aliaga-Alcalde, M. Soler, *Chem. Eur. J.* 22 (2016) 12808–12818.
- [25] I. Horcas, R. Fernández, J.M. Gómez-Rodríguez, J. Colchero, J. Gómez-Herrero, A.M. Baro, *Rev. Sci. Instrum.* 78 (2007) 013705–013708.
- [26] M. Martinez, N.J. Bruce, J. Romanowska, D.B. Kokh, M. Ozbovac, X. Yu, M.A. Oztürk, S. Richter, R.C. Wade, *J. Comput. Chem.* 36 (2015) 1631–1645.
- [27] W. Humphrey, A. Dalke, K. Schulten, *J. Mol. Graphics Modell.* 14 (1996) 33–38.
- [28] G. Brancolini, D.B. Kokh, L. Calzolari, R.C. Wade, S. Corni, *ACS Nano* 6 (2012) 9863–9878.
- [29] F. Iori, R. Di Felice, E. Molinari, S. Corni, *J. Comput. Chem.* 30 (2009) 1465–1476.
- [30] L.B. Wright, P.M. Rodger, S. Corni, T.R. Walsh, *J. Chem. Theory Comput.* 9 (2013) 1616–1630.
- [31] F. Iori, S. Corni, *J. Comput. Chem.* 29 (2008) 1656–1666.
- [32] H.J.J. Pabon, *Recl. Trav. Chim. Pays Bas* 83 (1964) 379–386.
- [33] U. Pedersen, P.B. Rasmussen, S.O. Lawesson, *Liebigs. Ann. Chem.* 1985 (1985) 1557–1569.
- [34] R.N. Moussawi, D. Patra, *RSC Adv.* 6 (2016) 17256–17268.
- [35] N. Aliaga-Alcalde, L. Rodríguez, M. Ferbinteanu, P. Höfer, T. Weyhermüller, *Inorg. Chem.* 51 (2012) 864–873.
- [36] R. Henriquez, L. Moraga, G. Kremer, M. Flores, A. Espinoza, R.C. Muñoz, *Appl. Phys. Lett.* 102 (2013) 051608.
- [37] V. Malyskyi, J.-J. Simon, L. Patrone, J.-M. Raimundo, *RSC Adv.* 5 (2015) 26308–26315.
- [38] *Handbook of X-ray Photoelectron Spectroscopy*, in: J.F. Moulder, W.F. Stickle, P.E. Sobol, K.D. Bomben, J. Chastain (Eds.), Perkin-Elmer Corporation, Eden Prairie, 1992.
- [39] H. Rieley, G.K. Kendall, F.W. Zemicael, T.L. Smith, S. Yang, *Langmuir* 14 (1998) 5147–5153.